

COHERENT 2018 at the Spallation Neutron Source

D. Akimov,^{1,2} J.B. Albert,³ P. An,^{4,5} C. Awe,^{4,5} P.S. Barbeau,^{4,5} B. Becker,⁶ V. Belov,^{1,2} M.A. Blackston,⁷ A. Bolozdynya,² A. Brown,^{8,5} A. Burenkov,^{1,2} B. Cabrera-Palmer,⁹ M. Cervantes,⁴ J.I. Collar,¹⁰ R.J. Cooper,¹¹ R.L. Cooper,^{12,13} J. Daughhetee,⁶ D.J. Dean,⁷ M. del Valle Coello,³ J.A. Detwiler,¹⁴ M. D'Onofrio,³ Y. Efremenko,⁶ S.R. Elliott,¹³ E. Erkela,¹⁴ A. Etenko,^{15,2} L. Fabris,⁷ M. Febbraro,⁷ N. Fields,¹⁰ W. Fox,³ A. Galindo-Uribarri,^{7,6} M.P. Green,^{16,5,7} M.R. Heath,³ S. Hedges,^{4,5} E.B. Iverson,⁷ M. Kaemingk,¹² L.J. Kaufman*,³ S.R. Klein,¹¹ A. Khromov,² S. Ki,^{4,5} A. Konovalov†,^{1,2} A. Kovalenko,^{1,2} A. Kumpan,² L. Li,^{4,5} W. Lu,⁷ K. Mann,^{16,5} Y. Melikyan,² D.M. Markoff,^{8,5} H. Moreno,¹² P.E. Mueller,⁷ P. Naumov,² J. Newby,⁷ D.S. Parno,¹⁷ S. Penttila,⁷ G. Perumpilly,¹⁰ D. Radford,⁷ R. Rapp,¹⁷ H. Ray,¹⁸ J. Raybern,^{4,7} D. Reyna,⁹ G.C. Rich‡,¹⁰ D. Rimal,¹⁸ D. Rudik,^{1,2} D.J. Salvat,¹⁴ K. Scholberg§,^{4,¶} B. Scholz,¹⁰ G. Sinev,⁴ W.M. Snow,³ V. Sosnovtsev,² A. Shakirov,² B. Suh,³ R. Tayloe,³ R.T. Thornton,³ I. Tolstukhin,³ J. Vanderwerp,³ R.L. Varner,⁷ C.J. Virtue,¹⁹ J. Yoo,²⁰ C.-H. Yu,⁷ and J. Zettlemoyer³

¹*Institute for Theoretical and Experimental Physics named by A.I. Alikhanov of National Research Centre Kurchatov Institute, Moscow, 117218, Russian Federation*

²*National Research Nuclear University MEPhI (Moscow Engineering Physics Institute), Moscow, 115409, Russian Federation*

³*Department of Physics, Indiana University, Bloomington, IN 47405, USA*

⁴*Department of Physics, Duke University, Durham, NC 27708, USA*

⁵*Triangle Universities Nuclear Laboratory, Durham, NC 27708, USA*

⁶*Department of Physics and Astronomy, University of Tennessee, Knoxville, TN 37996, USA*

⁷*Oak Ridge National Laboratory, Oak Ridge, TN 37831, USA*

⁸*Department of Mathematics and Physics, North Carolina Central University, Durham, NC 27707, USA*

⁹*Sandia National Laboratories, Livermore, CA 94550, USA*

¹⁰*Enrico Fermi Institute, Kavli Institute for Cosmological Physics and Department of Physics, University of Chicago, Chicago, IL 60637, USA*

¹¹*Lawrence Berkeley National Laboratory, Berkeley, CA 94720, USA*

¹²*Department of Physics, New Mexico State University, Las Cruces, NM 88003, USA*

¹³*Los Alamos National Laboratory, Los Alamos, NM, USA, 87545, USA*

¹⁴*Center for Experimental Nuclear Physics and Astrophysics,*

and Department of Physics, University of Washington, Seattle, WA 98195, USA

¹⁵*National Research Centre Kurchatov Institute, Moscow, 123182, Russian Federation*

¹⁶*Physics Department, North Carolina State University, Raleigh, NC 27695, USA*

¹⁷*Department of Physics, Carnegie Mellon University, Pittsburgh, PA 15213, USA*

¹⁸*Department of Physics, University of Florida, Gainesville, FL 32611, USA*

¹⁹*Department of Physics, Laurentian University, Sudbury, Ontario P3E 2C6, Canada*

²⁰*Department of Physics at Korea Advanced Institute of Science and Technology (KAIST) and Center for Axion and Precision Physics Research (CAPP) at Institute for Basic Science (IBS), Daejeon, 34141, Republic of Korea*

The primary goal of the COHERENT collaboration is to measure and study coherent elastic neutrino-nucleus scattering (CEvNS) using the high-power, $\mathcal{O}(10\text{-MeV})$, pulsed source of neutrinos provided by the Spallation Neutron Source (SNS) at Oak Ridge National Laboratory (ORNL). In spite of its large cross section, the CEvNS process is challenging to observe, due to tiny energies of the resulting nuclear recoils. The CEvNS cross section is cleanly predicted in the standard model of electroweak interactions; hence its measurement provides a new way to test the model. CEvNS is important for supernova physics and supernova-neutrino detection, and its measurement will enable validation of dark-matter detector background and detector-response models. Precision measurement of CEvNS will address questions of nuclear structure as well. The COHERENT collaboration reported the first detection of CEvNS [1] using a CsI[Na] detector. At present the

* Also at SLAC National Accelerator Laboratory, Menlo Park, CA 94205, USA

† Also at Moscow Institute of Physics and Technology, Institutsky Lane 9, Dolgoprudny, Moscow region, 141700, Russian Federation

‡ Formerly at Department of Physics and Astronomy, University of North Carolina at Chapel Hill, Chapel Hill, NC 27599, USA and Triangle Universities Nuclear Laboratory, Durham, NC 27708, USA

§ Corresponding author

collaboration is deploying four detector technologies: a CsI[Na] scintillating crystal, p-type point-contact germanium detectors, single-phase liquid argon, and NaI[Tl] crystals. All detectors are located in the neutron-quiet basement of the SNS target building at distances 20-30 m from the SNS neutrino source. The simultaneous measurement in all four COHERENT detector subsystems will test the N^2 dependence of the cross section and search for new physics. In addition, COHERENT is measuring neutrino-induced neutrons from charged- and neutral-current neutrino interactions on nuclei in shielding materials, which represent a non-negligible background for CEvNS as well as being of intrinsic interest. The Collaboration is planning as well to look for charged-current interactions of relevance to supernova and weak-interaction physics. This document describes concisely the COHERENT physics motivations, sensitivity and next plans for measurements at the SNS to be accomplished on a few-year timescale.

Contents

| | |
|---|----|
| I. Introduction | 2 |
| II. Coherent Elastic Neutrino-Nucleus Scattering Physics | 3 |
| A. Measurement of the N^2 -Dependent Cross Section | 3 |
| B. Beyond-the-Standard-Model Physics Searches | 5 |
| C. Relevance for Direct Dark Matter Detection Experiments | 6 |
| D. Future Physics with CEvNS | 7 |
| III. The COHERENT Experiment | 9 |
| A. Neutrinos at the Spallation Neutron Source | 9 |
| B. Background Studies | 10 |
| 1. Neutron Backgrounds | 10 |
| 2. Neutrino-Induced Neutron Backgrounds | 11 |
| C. Detector Subsystems | 12 |
| 1. CsI[Na] Detector Subsystem | 12 |
| 2. P-Type Point Contact HPGe Subsystem | 14 |
| 3. Single-Phase Liquid Argon Subsystem | 14 |
| 4. NaI[Tl] Subsystem | 15 |
| IV. COHERENT Status and Upgrades | 16 |
| A. Future Upgrades | 17 |
| V. Summary | 18 |
| References | 18 |

I. INTRODUCTION

Coherent elastic neutrino-nucleus scattering (CEvNS¹) was predicted in 1974 as a consequence of the neutral weak current [2, 3]. Although the cross section is large compared to other neutrino-matter interactions in the ~ 100 MeV energy range (see Fig. 1), this SM process took so long to be observed due to the daunting technical requirements: very low nuclear recoil energy thresholds, intense sources/large target

[¶]Electronic address: schol@phy.duke.edu

¹ Note there exist a number of abbreviations for this process in the literature, e.g., CNS, CNNS, CENNS. We favor a version with “E” for “elastic” to distinguish the process from inelastic coherent pion production, which is commonly confused with CEvNS by members of the high energy physics community. We prefer to replace the first “N” with “ν”, for “neutrino” because “NN” means “nucleon-nucleon” to many in the nuclear physics community. Finally, the Roman letter “v” standing in for the Greek letter “ν” can be pronounced as a “v”.

masses, and low backgrounds. Employing state-of-the-art low-energy-threshold detector technology coupled with the intense stopped-pion neutrino source available at the Spallation Neutron Source (SNS) at Oak Ridge National Laboratory (ORNL), the COHERENT Collaboration has made the first measurement of CEvNS [1], using neutrinos from pion decay at rest [4, 5]. The Collaboration has employed the data to search for physics beyond the standard model (SM). For the completion of the current phase, a suite of four detector subsystems (CsI[Na] scintillating crystals, p-type point-contact germanium detectors, a single-phase argon detector, and an array of NaI[Tl] scintillator detectors) will be deployed in the basement of the SNS, taking advantage of decades of detector development in the dark-matter direct-detection community. The immediate experimental impacts of the measurements envisioned with this detector suite include:

- Test of the SM prediction of proportionality of the CEvNS cross section to neutron number squared, N^2 .
- A precision cross-section measurement on multiple targets to test for non-standard neutrino interactions, for which the interaction depends on the quark makeup of the nucleus [5–7]. First constraints have already been made with the CsI[Na] measurement [1, 8–11] and future possibilities are described as well in reference [7].
- Systematic characterization of low-threshold recoil detectors with neutrinos to validate experimental background and detector-response models, given that CEvNS of solar and atmospheric neutrinos is an irreducible background for dark matter WIMP (Weakly Interacting Massive Particle) searches [12].
- Low-energy neutrino-scattering-based measurements of nuclear neutron distributions. An interpretation of the CsI[Na] measurement is given in Ref. [13].

Furthermore, the CEvNS process has one of the largest cross sections relevant for supernova dynamics and plays a significant role in core-collapse processes [14–16], and therefore should be measured to validate models of core-collapse supernovae. Dark-matter detectors will also be able to detect CEvNS interactions in the event of a nearby core-collapse supernova burst [17, 18], which will be sensitive to the full flavor content of the supernova signal.

As secondary goals, COHERENT will perform measurements of the charged-current (CC) and neutral-current (NC) cross sections $\text{Pb}(\nu_e, n)$, $\text{Fe}(\nu_e, n)$, and $\text{Cu}(\nu_e, n)$, which result in the emission of background-inducing fast neutrons. The measurement of this cross section on lead has implications for supernova neutrino detection in the HALO supernova neutrino detector [21]. These (ν, n) interactions may also influence nucleosynthesis in certain astrophysical environments [22, 23]. In addition, the NaI[Tl] detector array can be used to observe the CC reaction $^{127}\text{I}(\nu_e, e^-)^{127}\text{Xe}$ [24], which has relevance both for supernova physics and for g_A -quenching studies (see Sec. III C 4).

This paper describes the updated experimental configuration since Ref. [25], current status, near-future plans, and briefly, potential farther-future plans.

II. COHERENT ELASTIC NEUTRINO-NUCLEUS SCATTERING PHYSICS

The coherence of the CEvNS process results in an enhanced neutrino-nucleus cross section that is approximately proportional to N^2 , the square of the number of neutrons in the nucleus, due to the small weak charge of the proton. The coherence condition, in which the neutrino scatters off all nucleons in a nucleus in phase with each other, requires that the wavelength of the momentum transfer be larger than the size of the target nucleus. In this NC elastic process, initial and final states are the same. Substantial coherence requires low-energy neutrinos (typically < 50 MeV for medium- A nuclei); as a result, the experimental signature for the process is a difficult-to-detect keV to sub-keV nuclear recoil, depending on the nuclear mass and neutrino energy.

A. Measurement of the N^2 -Dependent Cross Section

The cross section for CEvNS can be written as:

$$\frac{d\sigma}{dT_{coh}} = \frac{G_F^2 M}{2\pi} \left[(G_V + G_A)^2 + (G_V - G_A)^2 \left(1 - \frac{T}{E_\nu}\right)^2 - (G_V^2 - G_A^2) \frac{MT}{E_\nu^2} \right] \quad (1)$$

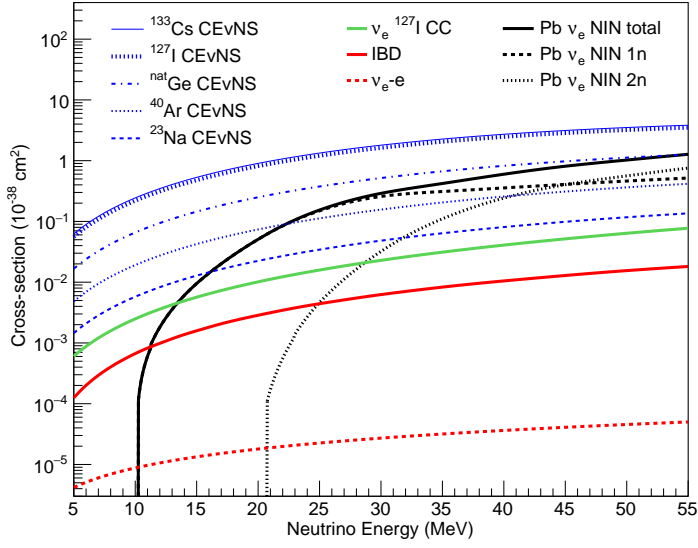


FIG. 1: Neutrino interaction cross sections per target as a function of neutrino energy for COHERENT target materials, as well as NIN cross sections on lead (see Sec. III B 2). Also shown, to compare with other cross sections in this energy range, are the ν_e CC cross section on ^{127}I [19, 20] and the frequently-used cross sections for inverse beta decay of $\bar{\nu}_e$ on free protons (IBD) and elastic scattering of ν_e on electrons (per electron).

$$G_V = (g_V^p Z + g_V^n N) F_{\text{nucl}}^V(Q^2) \quad (2)$$

$$G_A = (g_A^p (Z_+ - Z_-) + g_A^n (N_+ - N_-)) F_{\text{nucl}}^A(Q^2), \quad (3)$$

where G_F is the Fermi constant, M is the nuclear mass, T is the recoil energy, E_ν is the neutrino energy, $g_V^{n,p}$ and $g_A^{n,p}$ are vector and axial-vector coupling factors, respectively, for protons and neutrons, Z and N are the proton and neutron numbers, Z_\pm and N_\pm refer to the number of up or down nucleons, and Q is the momentum transfer [26]. The maximum recoil energy for a given target species and neutrino energy is $T_{\text{max}} = \frac{2E_\nu^2}{M+2E_\nu}$. The form factors $F_{\text{nucl}}^{A,V}(Q^2)$ are point-like ($F(Q^2) = 1$) for interactions of low-energy neutrinos < 10 MeV, but suppress the interaction rate as the wavelength of the momentum transfer becomes comparable to the size of the target nucleus (i.e., for higher neutrino energies and for heavier targets). The vector couplings appearing in G_V and G_A are written as:

$$g_V^p = \rho_{\nu N}^{NC} \left(\frac{1}{2} - 2\hat{\kappa}_{\nu N} \sin^2 \theta_W \right) + 2\lambda^{uL} + 2\lambda^{uR} + \lambda^{dL} + \lambda^{dR} \quad (4)$$

$$g_V^n = -\frac{1}{2}\rho_{\nu N}^{NC} + \lambda^{uL} + \lambda^{uR} + 2\lambda^{dL} + 2\lambda^{dR}, \quad (5)$$

where $\rho_{\nu N}^{NC}$, $\hat{\kappa}_{\nu N}$ are electroweak parameters, $\lambda^{uL}, \lambda^{dL}, \lambda^{dR}, \lambda^{uR}$ are radiative corrections given in Refs. [26, 27], and θ_W is the weak mixing angle. Figure 1 shows CEvNS cross sections as a function of neutrino energy, and Fig. 2 shows the expected CEvNS cross section weighted by stopped-pion neutrino flux (see Section III A), as a function of N , with and without form-factor suppression. The deployment of the COHERENT detector suite in “Neutrino Alley”, a basement location at the SNS, which is ~ 20 m from the source of neutrinos, has resulted in one measurement [1], and measurements with additional targets will result in a clear observation of the coherent N^2 nature of the cross section (Fig. 2). The expected precisions of the cross section measurements will quickly become dominated by the systematic uncertainty of the knowledge of the nuclear recoil detector thresholds (see Sec. IV) and neutrino flux uncertainties. Threshold uncertainties are dominant for the heavier Cs and I nuclei due to the lower average recoil energies for these species.

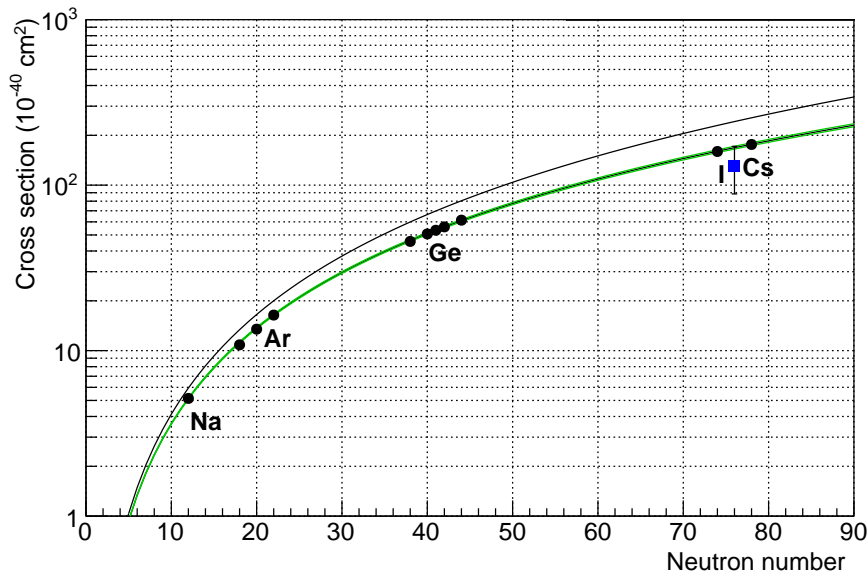


FIG. 2: Illustration of the $\propto N^2$ proportionality of the stopped-pion-neutrino flux-averaged CEvNS cross section versus neutron number N . The black line assumes a unity form-factor. The green band shows the effect of an assumed form factor (very similar effects from [28, 29] and [30], the latter used in the prediction in Ref. [1]), with its width indicating the effect of a $\pm 3\%$ uncertainty on the assumed neutron rms radius in the Helm parameterization. The points show the the relevant isotopes of COHERENT target materials. The blue square shows the flux-averaged cross section inferred from the measurement reported in Ref. [1].

The expected recoil spectra before detection-efficiency corrections are shown in Fig. 3.

B. Beyond-the-Standard-Model Physics Searches

Because the CEvNS cross section is cleanly predicted in the SM, deviations can indicate new physics (e.g., [6, 26, 32–34]). As one example of a test of beyond-the-SM physics, the CEvNS cross section for even-even nuclei, incorporating possible non-standard-interaction (NSI) neutral currents, can be parameterized as:

$$\frac{d\sigma}{dT_{coh}} = \frac{G_f^2 M}{2\pi} G_V^2 \left[1 + \left(1 - \frac{T}{E_\nu} \right)^2 - \frac{MT}{E_\nu^2} \right] \quad (6)$$

$$G_V = ((g_V^p + 2\epsilon_{ee}^{uV} + \epsilon_{ee}^{dV}) Z + (g_V^n + \epsilon_{ee}^{uV} + 2\epsilon_{ee}^{dV}) N) F_{\text{nucl}}^V(Q^2), \quad (7)$$

where the ϵ 's represent new couplings [5, 26]; hence CEvNS is a novel probe of new mediators. Neutrino-scattering constraints on the magnitude of non-zero values for ϵ_{ee}^{qV} from CHARM [35] are of order unity; they are shown in Fig. 4 as the shaded grey region². A further search for NSI can be performed by comparing measured CEvNS cross sections to SM expectations. CEvNS constraints may also help to resolve NSI ambiguities for interpretation of neutrino oscillation parameter measurements [7, 36]. The initial NSI result from COHERENT [1] for two parameters, ϵ_{ee}^{uV} and ϵ_{ee}^{dV} (assuming all other ϵ parameters are zero) is shown in Fig. 4 as a blue band. Reference [8] shows that the first data set can already constrain the “LMA-D”

² Note that these constraints are valid only for mediators not much lighter than the electroweak scale [7].

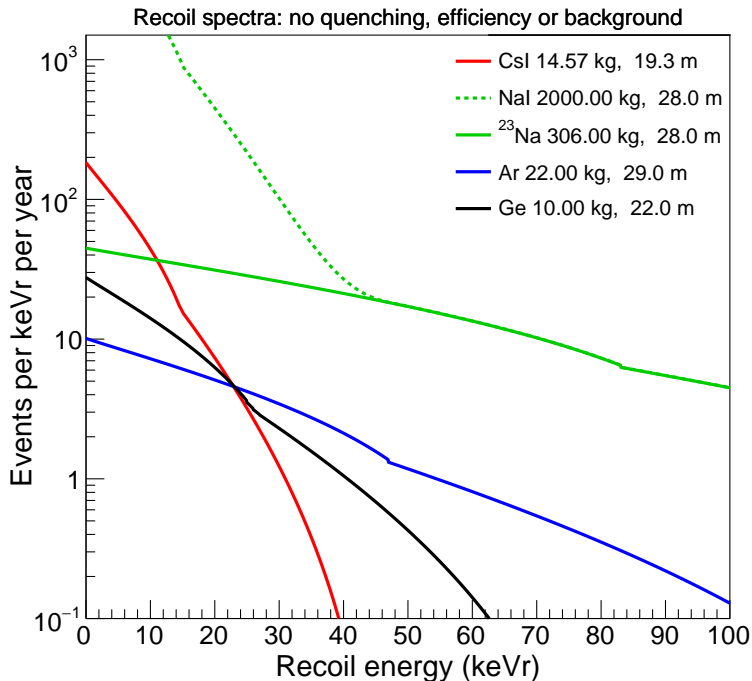


FIG. 3: Differential recoil rates for the COHERENT suite of detectors in Neutrino Alley. This plot represents interaction rates for the first 6000 ns after each beam pulse, including all flavors and assuming 100% detection efficiency. Note this does not take into account quenching factors, which are different for different detectors, or other detector-specific efficiencies. The kinks are due to different endpoints of prompt and delayed flavor components for different target isotope components. The contribution from ^{23}Na to NaI is shown separately, as the small quenching factor for ^{127}I in NaI [31] is likely to strongly suppress the ^{127}I contribution to the observed rate. The materials are assumed to have natural abundances of isotopes.

degeneracy. Sensitivity to NSI parameters can be improved with simultaneous measurements of the cross sections on different nuclei that factor out the neutrino flux uncertainty. The angles of the diagonal-band allowed regions vary slightly between the different isotopes due to different $N : Z$ ratios. With realistic parameters for the current phase of COHERENT, described in the section below, the expected constraints from a null search for CsI[Na], Ge, Ar, NaI[Tl], and the combined analysis, are shown in Fig. 4 as superimposed diagonal bands, along with a projection for long-term scenario with small systematic uncertainties to illustrate future potential. CEvNS measurements using stopped-pion neutrinos can also constrain other NSI parameters. Precision measurements of the CEvNS recoil spectrum also provide information on potential beyond-the-SM couplings [9]. Examples of constraints from the CsI[Na] data set, and future potential, are described further in Refs. [8–10].

C. Relevance for Direct Dark Matter Detection Experiments

CEvNS has long been closely linked to direct dark matter searches [4, 37]. The CEvNS of solar and atmospheric neutrinos, which produce single-scatter recoils identical to those expected from WIMPs, is recognized as an irreducible background for dark-matter WIMP searches for next-generation dark-matter experiments [12, 38–42]; see Fig. 5. Large dark-matter detectors may eventually be able to address solar neutrino physics using CEvNS [4, 43].

The four detector technologies and materials proposed within the COHERENT program overlap well with those in use by the WIMP community. Existing and next-generation experiments such as DarkSide [44] and DEAP [45] use argon detectors; SuperCDMS [46], EDELWEISS [47], and CDEX [48] use germanium

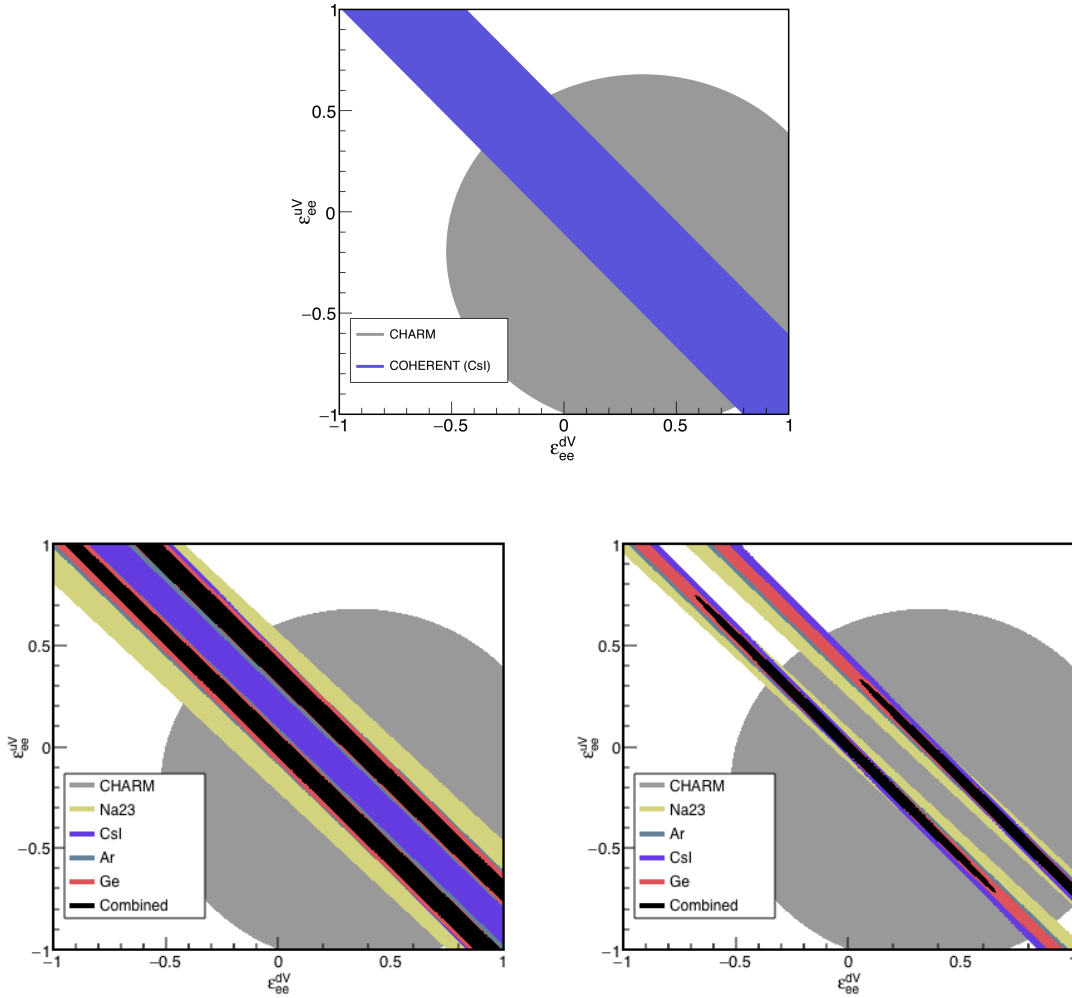


FIG. 4: Top: result from [1] with initial constraints on two of the NSI ϵ parameters, showing also the constraint from the CHARM experiment [35]. Bottom left: same with realistic assumptions for COHERENT’s detector suite for the next three years. Assumptions on mass, distance and threshold are given in Table I (assuming 2 tonnes of NaI, ^{23}Na component only, first 1000 ns of the beam window for Na and first 6000 ns for the others). The black shows the result from a combined fit. Bottom right: predicted sensitivity obtained with the COHERENT detector materials, with 5% uncertainties on flux and event rates and assuming systematically-limited measurements.

detectors; DAMA/LIBRA [49], DMIce [50], SABRE [51] and COSINE [52] use NaI detectors; and the KIMS collaboration is conducting a WIMP search with CsI(Tl) crystals [53]. By utilizing the intense SNS neutrino source, COHERENT can provide detector-specific response information for CEvNS interactions as a supplement to other low-energy calibration techniques. A further constraint on cross-section uncertainty is afforded by the presence of higher-energy ($\gtrsim 10$ MeV) neutrinos in the SNS beam: these neutrinos will be a unique probe of nuclear form factors.

D. Future Physics with CEvNS

Beyond the scope of this first suite of detectors, a successful CEvNS program will enable new endeavors addressing further physics questions in the long term.

Of particular note is that the weak mixing angle (θ_W) appears in the vector coupling factors of Eq. 1. It

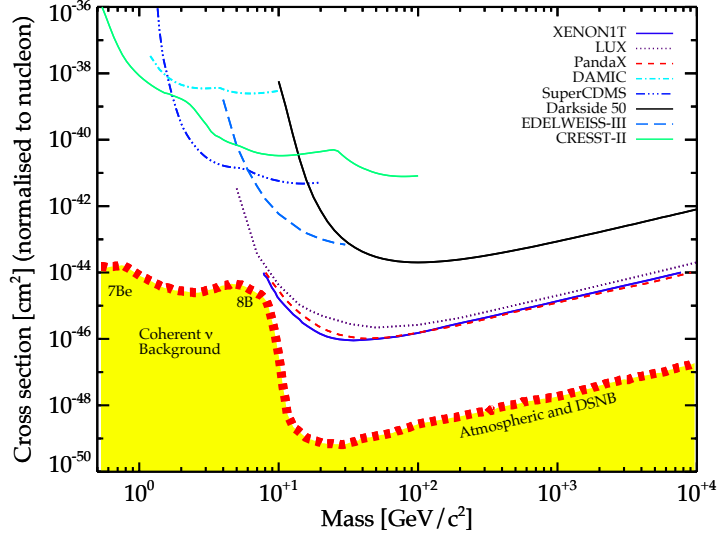


FIG. 5: WIMP dark-matter search parameter space, showing “neutrino floor” from CEvNS of solar, diffuse relic and atmospheric neutrinos as a thick dashed orange line, relevant for spin-independent WIMP-nucleon interactions. (Figure courtesy of L. Strigari, updated from [12].)

has long been predicted that a precision measurement of the CEvNS cross section would provide a sensitive test of the weak nuclear charge and of physics above the weak scale [32]. Theoretical uncertainties are very small. In addition to the terms in Eq. 1, there also exist axial-vector terms from strange quark and weak magnetism contributions for non-even-even nuclear targets that have larger theoretical uncertainties (as much as 5% uncertainty for light nuclei for larger Q). For the even-even targets we are considering, these uncertainties are $< 0.1\%$. For ^{23}Na (and possibly other targets), however, the axial contribution may be measurable. While the total neutrino flux uncertainty is estimated to be $\sim 10\%$, improvements using multiple targets to cancel uncertainties will permit few-percent or better measurements of $\sin^2 \theta_W$.

CEvNS offers a measurement of the weak mixing angle at $Q \sim 40 \text{ MeV}/c$, where there is sensitivity to models of dark Z bosons, which offer a possible explanation for the $(g-2)_\mu$ anomaly [54, 55] and a glimpse into dark sector physics [56–59]. A CEvNS measurement interpreted simply as a determination of $\sin^2 \theta_W$ has substantially larger uncertainty than those from parity-violating electron scattering experiments (see [60] for a comprehensive review). However, CEvNS measurements will be subject to different systematic uncertainties and provides an independent reckoning at comparable values of momentum transfer. Furthermore, the Q^2 dependence of the CEvNS recoil spectrum offers a stringent test of models explaining the $(g-2)_\mu$ anomaly, with the first CsI[Na] measurement already ruling out an extensive range of currently-allowed parameters [9].

Additional examples of future CEvNS physics include:

- A measurement of the CEvNS interaction spectrum is sensitive to the magnitude of the neutrino magnetic moment [5, 61, 62] resulting in a characteristic enhancement of low-energy recoils. Because the neutrino magnetic moment is predicted to be extremely tiny in the SM, a measurement of non-zero magnetic moment would indicate new physics. A stopped-pion flux allows access to measurements with ν_μ flavor [5].
- Precision measurement of the ratio of the muon and electron neutrino cross sections ($\sim \text{few } \%$), which can be done by comparing prompt (ν_μ) and delayed ν_e stopped-pion signals, will be sensitive to the effective neutrino charge radius [63].
- Development of this flavor-blind NC CEvNS detection capability will provide a natural tool to search for oscillations into sterile neutrinos in near and far detectors [4, 64].
- The neutron distribution function (nuclear form factor) can be probed with measurements of the CEvNS recoil spectrum [65, 66]. Incoherent contributions to the cross section are also of interest for

study of nuclear axial structure [67]. Reference [13] determines the neutron rms radius for CsI to 18% using the 2017 CsI[Na] result, although without taking into account spectral shape uncertainties.

- A $\mathcal{O}(1 \text{ tonne})$ Ar or other future COHERENT recoil-sensitive detector would be sensitive to sub-GeV particles postulated in some models as candidate dark matter [68, 69]. Such light, weakly-coupled particles could be produced via pion decays in the 1-MW proton target and would interact coherently with nuclei in the detector.

III. THE COHERENT EXPERIMENT

The COHERENT Collaboration has assembled a suite of detector technologies suitable for the observation of CEvNS at the SNS. The SNS is the highest-flux pulsed, stopped-pion neutrino source currently available. This effort leverages the technological development within the dark-matter direct-detection community over the last decade by deploying four mature low-threshold/low-background technologies (with five elemental targets) capable of observing low-energy nuclear recoils: CsI[Na] scintillating crystal, p-type point-contact (PPC) germanium detectors, single-phase liquid argon, and NaI[Tl] scintillating crystals. The use of targets with widely varying numbers of neutrons provides a ready test of the N^2 nature of the cross section and allows a convenient cross-check on the measured cross section given that detectors are subject to systematic response (quenching factor, QF) uncertainties. All four detector subsystems inhabit the Neutrino Alley hallway where a background measurement campaign (see Sec. III B) has indicated very low beam-related neutron backgrounds. In this section we will describe the properties of the SNS neutrino source, the results of background measurements, and the detectors.

A. Neutrinos at the Spallation Neutron Source

A stopped-pion beam has several advantages for CEvNS detection. First, the relatively high energies enhance the cross section ($\propto E^2$) while still benefiting from coherence; cross sections at stopped-pion energies (up to 50 MeV) are about two orders of magnitude higher than at reactor energies ($\sim 3 \text{ MeV}$). Second, recoil energies (few to tens of keV) bring detection of CEvNS within easy reach of the current generation of low-threshold detectors. Finally, the different flavor content of the SNS flux (ν_μ , ν_e and $\bar{\nu}_\mu$) means that physics sensitivity is complementary to that for reactor experiments (which have $\bar{\nu}_e$ only).

The SNS produces an intense, isotropic stopped-pion neutrino flux, with a sharply-pulsed timing structure that is highly beneficial for background rejection and precise characterization of the backgrounds not associated with the beam [70]. See Fig. 6.

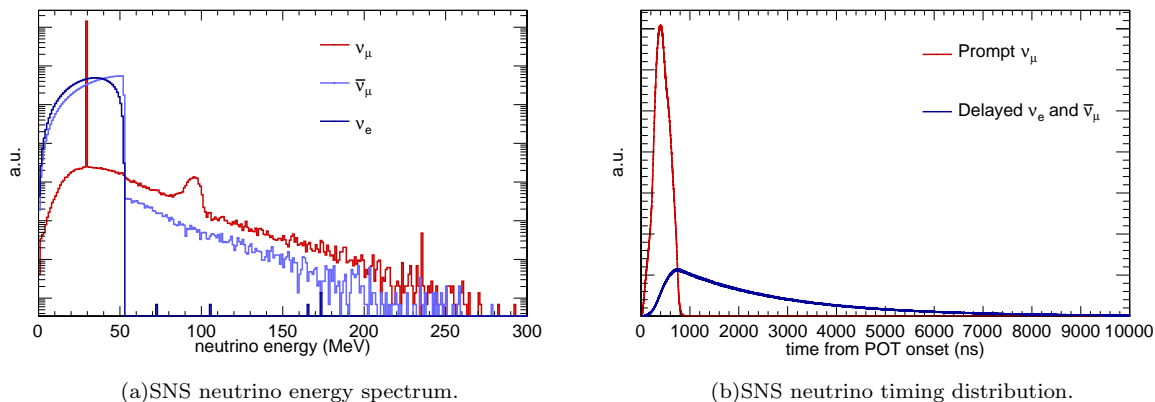


FIG. 6: (a) Expected ν spectrum at the SNS, showing the very low level of decay-in-flight and other non-decay-at-rest flux, in arbitrary units; the integral is 4.3×10^7 neutrinos/cm²/s at 20 m. (b) Time structure for prompt and delayed neutrinos due to the 60-Hz pulses. “Prompt” refers to neutrinos from pion decay, and “delayed” refers to neutrinos from muon decay.

A neutrino flux simulation has been developed for neutrino experiments at the SNS using GEANT4.10.1 [71]. Using this code, a beam of mono-energetic 1-GeV protons impinges upon a liquid mercury target. For the baseline simulation, a simplified version of the SNS target geometry was implemented. Neutrino spectra and flux are recorded for a COHERENT detector in the basement, 20 m from the target center at an angle of -110° with respect to the proton beam direction. Resulting neutrino spectra and time distributions for different GEANT4 physics lists were compared; good agreement was found between “QGSP_BERT” and “QGSP_INCLXX” physics lists. The flux prediction corresponding to QGSP_BERT is used for the signal predictions shown here. See the supplemental materials of Ref. [1] for more details.

The results of the simulations show that the contributions to the neutrino spectrum from decay-in-flight and μ -capture are expected to be very small (Fig. 6). The contribution to the CEvNS signal from these high-energy neutrinos ($E > 50$ MeV) is $< 1\%$. This contamination is at least two orders of magnitude smaller than at other existing facilities, e.g., at Fermilab [72] and J-PARC [73, 74]. The SNS neutrino flux is also ~ 80 times larger than that at the Fermilab Booster Neutrino Beam at the same distance from the source. The overall uncertainty on the neutrino flux is estimated to be 10% [1].

B. Background Studies

Understanding and reducing sources of background are critical requirements of the COHERENT experimental program. The short SNS duty cycle will reduce steady-state backgrounds due to radioactivity and cosmogenics by a factor of $10^3 - 10^4$. Steady-state backgrounds can also be understood using data taken outside the SNS beam window; however, beam-related backgrounds, especially fast neutrons, will be evaluated using ancillary measurements (described below) and modeling.

1. Neutron Backgrounds

A background measurement campaign has been underway since the fall of 2013. Several detection systems have been used to measure beam-related neutron backgrounds, including: a single portable 5-liter liquid-scintillator detector to assess gross neutron rates at various locations within the SNS target hall and basement, a two-plane neutron scatter camera [75] to provide detailed neutron spectra and some directional information (Fig. 8(a)), and a single-plane liquid-scintillator array to provide systematic cross-checks of the neutron scatter camera data. The measurements taken to date indicate that Neutrino Alley is very neutron-quiet; the direct beam-related neutrons are more than four orders of magnitude lower in the basement than on the experimental floor of the SNS (see Fig. 7). The location is also protected from cosmic rays by ~ 8 meters-water-equivalent (m.w.e.) of overburden. The measured backgrounds in the basement are used to estimate the beam-related backgrounds for all detector subsystems.

The neutron scatter camera took data at several positions in Neutrino Alley. In addition, ancillary measurements were performed with the complementary SciBath detector [72, 76, 77] (Fig. 8(b)), a liquid-scintillator tracking detector. The combination of the two provided a systematic cross-check, increasing confidence in the understanding of the neutron background energy spectra.

Beam-related neutron backgrounds can be addressed effectively by taking advantage of the timing characteristics of the SNS (illustrated in Fig. 6). The SNS provides beam timing signals that allow precise selection around the $\lesssim 800$ -ns-width arrival time of protons on target. While a small background contribution from beam-related neutrons is expected to add to the ν_μ signal in the “prompt” window (coincident with protons on target), all neutron background measurements indicate that there are negligible beam-related neutrons expected in the “delayed” window, when the ν_e and $\bar{\nu}_\mu$ from muon decay arrive.

Acceptance and efficiency corrections to the measured neutron scatter camera spectra were performed in order to provide useful background estimates for the detector subsystem simulations (Fig. 7). The flux measurements are dominated by uncertainties due to variations in the angular acceptance of the neutron scatter camera (factors of 3–5). For the CsI[Na] measurement, neutron backgrounds were evaluated in-situ [1] using a scintillator cell inside the shielding, and in addition were constrained by the absence of inelastic neutron scattering signals from the crystal.

To maintain confidence in the understanding of the neutron backgrounds, continued additional measurements are underway. The Multiplicity and Recoil Spectrometer (MARS) apparatus [78] (Fig. 8(c)), a

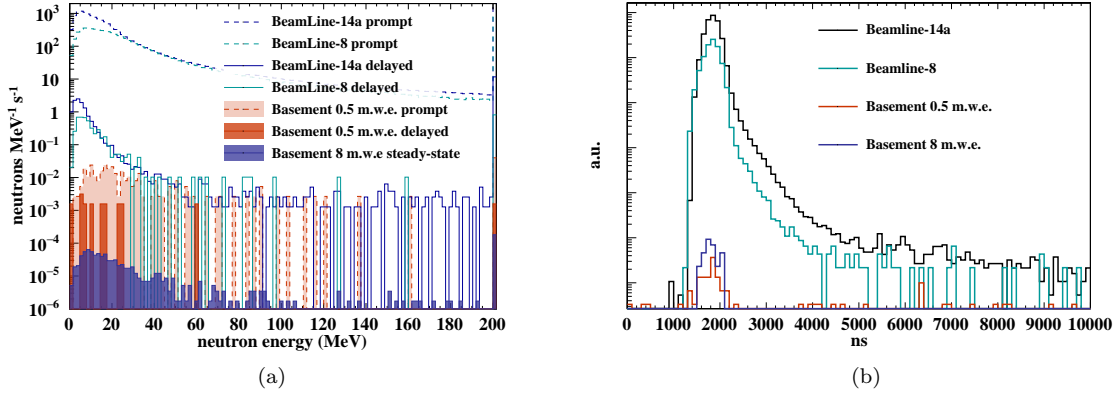


FIG. 7: (a) Fast neutron spectra measured with the neutron scatter camera throughout the SNS facility. A clear reduction by over four orders of magnitude from the experimental hall to the basement locations is seen. No neutron scatters were detected in the delayed window for the basement 8 m.w.e. location. (b) Arrival times of neutrons with respect to SNS beam timing signals. The proton pulse time offset with respect to zero is 1400 ns.

transportable fast neutron spectrometer using Gd-doped scintillator, is currently under commissioning in Neutrino Alley.

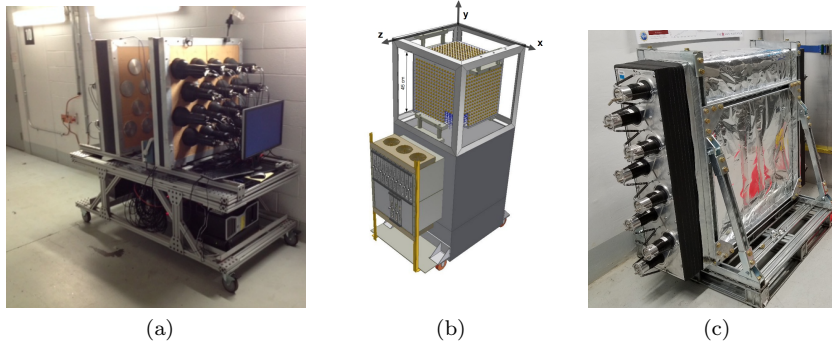


FIG. 8: (a) The neutron scatter camera deployed in the SNS basement. (b) The SciBath detector. (c) The MARS detector.

2. Neutrino-Induced Neutron Backgrounds

The high-energy neutrinos from pion decay at rest have energies above the neutron separation threshold in ^{208}Pb , a ubiquitous material in detector radiological shields. The CC interaction ($^{208}\text{Pb}(\nu_e, e^-)^{208}\text{Bi}$), with subsequent prompt neutron emission, may produce significant numbers of *background-producing* neutrons in the Pb shields, pulsed in time with the beam and sharing the $2.2\text{-}\mu\text{s}$ characteristic time-structure of the ν_e due to the muon lifetime. Other isotopes of Pb should have similarly large neutron-ejection cross sections, and other elements commonly used for shielding (Fe, Cu) may also produce neutrino-induced neutrons (NINs) in CC and NC reactions.

The NIN cross section is estimated theoretically only within a factor of ~ 3 [79–81]; the only measurement for these targets in this energy range is an inclusive CC $^{56}\text{Fe}(\nu_e, e^-)^{56}\text{Co}$ measurement [82]. Therefore, a careful measurement of the NIN production cross section is of great importance for background predictions. The measurement of these cross sections also has an impact on the ongoing HALO supernova neutrino detection experiment [21, 83]. The spallation of neutrons from heavy elements is also expected to influence

the nucleosynthesis of heavy elements in supernovae [22, 23].

The COHERENT liquid-scintillator-cell measurement inside the CsI shielding favors a non-zero NIN signal at 2.9σ [1], although it also suggests a smaller cross section than from theoretical expectation. Dedicated apparatuses for NIN measurement containing liquid-scintillator detectors surrounded by lead or other target materials and further surrounded by a muon veto and neutron moderator were designed and deployed to the SNS basement in September 2015 (see Figure 9). These detector systems, currently running with lead and iron, are expected to continue operation through the lifetime of the experiment. COHERENT will use these to measure the production cross sections of NINs in lead, iron, and copper at the SNS, both to evaluate the NIN background for CEvNS and as independent physics measurements.

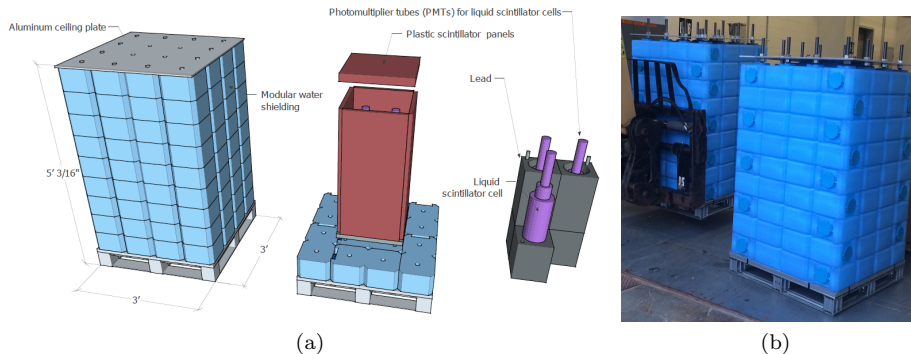


FIG. 9: (a) Schematic drawing of the detectors to measure the neutrino-induced neutron cross section on Pb, Fe, and Cu. (b) The imperfectly-named “Neutrino Cubes,” or “NIN Cubes,” modular neutrino-induced neutron experiments.

C. Detector Subsystems

The COHERENT Collaboration is deploying four detector subsystems, each containing different target nuclei (summarized in Tab. I). The timing resolution of all four detector subsystems is sufficient to allow the observation of the characteristic $2.2\text{-}\mu\text{s}$ lifetime of muon-decay neutrinos, a further cross-check that any interactions are due to neutrinos from the SNS. The technologies are mature and all are presently used for direct dark-matter detection or other low-threshold experiments.

Fig. 10 shows the current COHERENT siting in Neutrino Alley.

| Nuclear target | Technology | Mass (kg) | Distance from source (m) | Recoil threshold (keVnr) |
|----------------|-----------------------|-----------|--------------------------|--------------------------|
| CsI[Na] | Scintillating crystal | 14.6 | 19.3 | 6.5 |
| Ge | HPGe PPC | 10 | 22 | 5 |
| LAr | Single-phase | 22 | 29 | 20 |
| NaI[Tl] | Scintillating crystal | 185*/2000 | 28 | 13 |

TABLE I: Parameters for the four COHERENT detector subsystems. *NaI[Tl] deployed in high-threshold mode is described in Sec. III C 4.

1. CsI[Na] Detector Subsystem

CsI[Na] scintillators (cesium iodide crystals doped with sodium) present several advantages for a CEvNS measurement. This mature technology combines sufficiently low thresholds with large neutron numbers ($N = 74, 78$) that make an observation of this process at the SNS feasible. Both recoiling species are essentially indistinguishable due to their very similar mass, greatly simplifying understanding the detector response. CsI is a rugged, room-temperature detector material, and is also relatively inexpensive ($\sim \$1/\text{g}$). These detectors

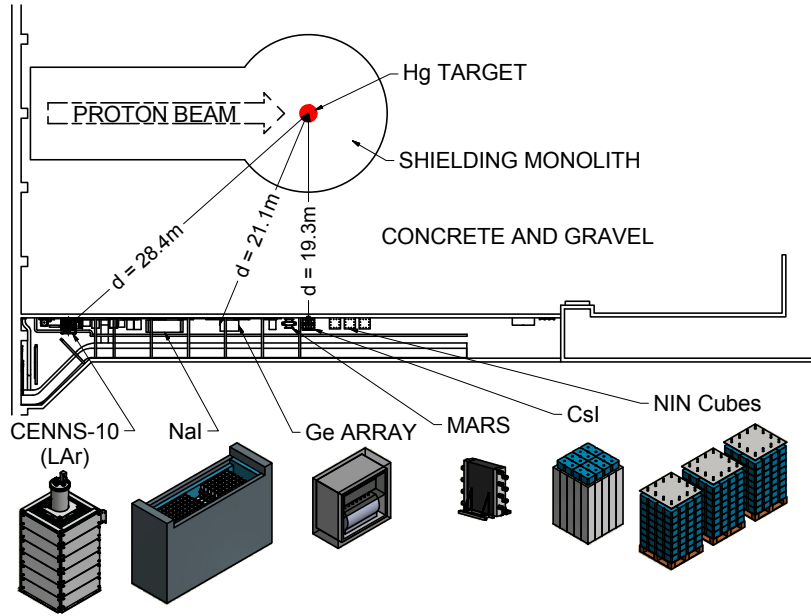


FIG. 10: Siting of existing and near-future planned detectors in Neutrino Alley.

have several other practical advantages. CsI[Na] exhibits a high light yield of 64 photons/keVee (electron-equivalent energy deposition) and has the best match to the response curve of bi-alkali photomultipliers of any scintillator material. CsI[Na] also lacks the excessive afterglow (phosphorescence) that is characteristic of CsI[Tl] [84], an important feature in a search involving small scintillation signals in a detector operated at ground level. The quenching factor for nuclear recoils (the fraction of the recoil energy that is detectable as scintillation) in this material over the energy region of interest has been carefully characterized [84], using the methods described in [31]. The quenching factor has been measured by the Collaboration using quasi-monochromatic neutron beams [1].

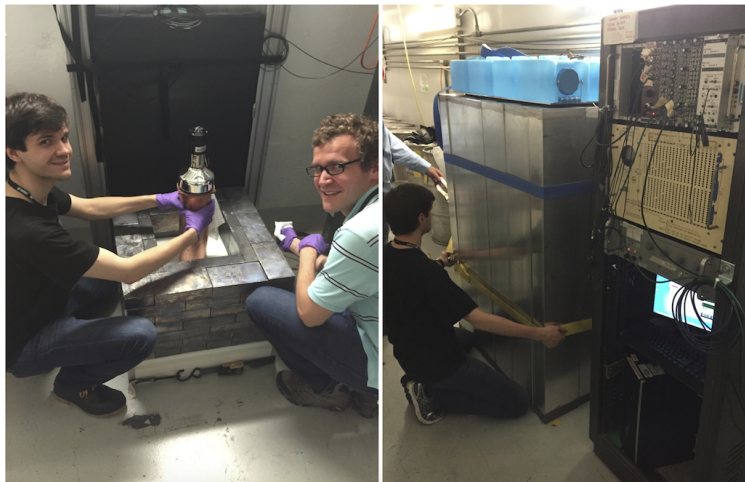


FIG. 11: The installation of the 14.6-kg, low-background CsI[Na] at the SNS (featuring B. Scholz [85] and G. Rich [86]). Successive layers of shielding include (inside-to-out): 7.62 cm HDPE, 15 cm of lead, a 5-cm thick muon veto and 10 cm of water neutron moderator.

A 14.57-kg CsI[Na] detector and shielding (Fig. 11) was characterized at the University of Chicago and

installed at the SNS in June 2015. The shielding consists of HDPE inner neutron moderator, Pb (the innermost 5 cm selected for low ^{210}Pb content), a 99.6%-efficient muon veto, and an outer neutron moderator and absorber. See reference [84] for more details of the detector and its characterization, as well as references [1, 85, 86] for details of the deployment and analysis of the 2015-2017 dataset resulting in the first observation of CEvNS. Continued running will bring improved statistical uncertainty, and analysis improvements are underway to improve signal to background ratio.. The uncertainty on the predicted rate is currently dominated by quenching factor uncertainties, which can be reduced by ancillary measurements.

2. P-Type Point Contact HPGe Subsystem

P-type point contact (PPC) germanium detectors display a set of unique properties in a large-mass (up to few kg) radiation detector: excellent energy resolution, sensitivity to energy depositions well below 1 keVee, and the intrinsic radiopurity that characterizes detector-grade (HPGe) germanium crystals. Following their description in [87, 88], PPCs have been adopted by a number of searches in dark matter and neutrino physics: CoGeNT (Coherent Germanium Neutrino Technology) [89–92], the MAJORANA DEMONSTRATOR [93], GERDA [94], CDEX [48], TEXONO [95], and most recently CONUS [96, 97]. Continuous development over the course of the past decade has enabled the reproducible manufacture of detectors with masses of up to 2.5 kg, while maintaining an intrinsic electronic noise of ~ 75 eV FWHM, equivalent to an energy threshold of ~ 150 eVee. Taking into consideration the measured quenching factor for nuclear recoils in germanium, this allows for detection of recoils with energy below 1 keVnr. In addition to extremely low energy thresholds, the low noise and 3-eV band-gap energy gives these detectors an excellent energy resolution near threshold. As a result, the measured (background-subtracted) energy-deposition spectrum is faithful to the true recoil spectrum, allowing for straightforward searches for deviations of the recoil spectrum due to nuclear form factors or new physics.

The COHERENT Collaboration aims to deploy a 10-kg array of PPC germanium detectors at the SNS for an initial measurement of CEvNS in germanium and to potentially probe new physics. COHERENT collaborators have access to 10 kg of existing Canberra BEGe PPCs, which are currently undergoing refurbishment and being evaluated for internal backgrounds in their original manufacturer-supplied cryostats for potential deployment at the SNS in 2018. While these on-hand detectors may be capable of an initial CEvNS measurement, they are not representative of the current technological capability in terms of threshold (~ 1 keVee as opposed to ~ 150 eVee) or low-background cryostat fabrication. An array of four state-of-the-art detectors, each with masses of ~ 2.5 kg and thresholds comparable to the lowest achieved to date, is being planned for potential deployment at the SNS with the aim of not only sensitively measuring the CEvNS spectrum, but doing so with a recoil energy threshold low enough to probe electromagnetic properties of neutrinos.

3. Single-Phase Liquid Argon Subsystem

The intended first phase of the experiment, proposed in Ref. [25], included a two-phase liquid xenon detector [98]. This detector could not be made available to COHERENT for this measurement, so an alternative plan utilizing a single-phase liquid argon detector was developed. Argon has been proposed for CEvNS measurements at stopped-pion neutrino sources [72, 99] in the past. It represents a relatively small value of N and a high fraction of the zero-spin isotope ^{40}Ar . The scintillation light yield at 128 nm is high (~ 40 photons per keVee). The different time constants of singlet and triplet molecular decay channels permit pulse-shape discrimination of nuclear recoils from electronic recoils [100]. Like other noble liquids, it is naturally clean of radioactive impurities, although it does contain ~ 1 Bq/kg of the long-lived cosmogenic isotope ^{39}Ar which decays via a 565-keV β . However, pulse-shape discrimination together with the pulsed SNS beam provides suppression of steady-state backgrounds.

The currently-installed LAr detector (Fig. 12) [101] began as the ‘‘CENNS-10’’ prototype detector built at Fermilab [72], tested and modified at Indiana University, then installed with the requisite shielding in Neutrino Alley at the SNS in December 2016. It consists of a cylindrical 56.7-liter LAr chamber, viewed by two 8’’ Hamamatsu R5912-02MOD photomultiplier tubes (PMTs) on opposite ends. The sides of the cylinder are lined by a tetraphenyl butadiene (TPB)-coated reflector. This originally consisted of an acrylic cylinder 27 cm diameter by 46 cm in length backed by a Teflon sheet. Acrylic disks were placed at the

cylinder ends in front of the PMTs. In June 2017, the acrylic cylinder was replaced with a 21-cm diameter Teflon cylinder, the acrylic end disks were removed and two new PMTs (of same type) with TPB directly coated on the front surface were installed. The active fiducial volume was reduced from 32 kg to 22 kg but it is expected that the light yield improve will compensate. The LAr is liquefied and maintained at temperature with a single-stage pulse-tube cold head cryorefrigerator. The boiloff Ar gas is recirculated through a Zr getter to remove N_2 to the ~ 10 -ppm level. The goal is to obtain several collected photoelectrons per keV for electronic recoils which, with a nuclear recoil response of ~ 0.25 [102], should allow an energy threshold of ~ 20 keV for CEvNS nuclear recoil events.

The detector shielding structure was designed to lower the rate of neutron and photon backgrounds. It consists of an inner water tank providing ~ 22 cm of water surrounded by 0.6 cm of copper, 10 cm of external lead, and stabilized with 0.6 cm aluminum plates. Simulations indicate that this structure will reduce the background rate well below that of the 20-100 keV CEvNS nuclear recoil.

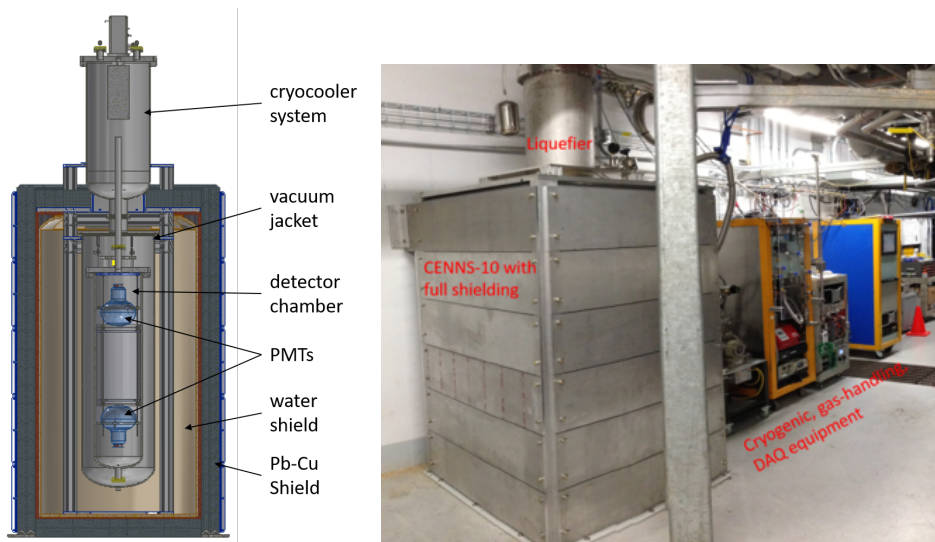


FIG. 12: Left: Liquid Ar detector section-view schematic. Right: Liquid Ar detector and associated equipment in Neutrino Alley.

4. NaI[Tl] Subsystem

NaI[Tl] is another material with capacity for low-threshold recoil detection. The sole stable sodium isotope, ^{23}Na , with 12 neutrons, has the lowest N value of COHERENT's target materials, and hence will result in the highest-energy recoils. A small- N nuclear target in combination with measurements on heavier nuclides reduces the impact of the flux uncertainty and improves physics reach (see Sections II B, II D). Furthermore, a few-percent effect from axial contributions is expected at high recoil energy, and could be of interest to measure in the longer term. The light yield is ~ 40 photoelectrons per keV.

About ~ 2 tonnes of recycled NaI[Tl] detectors are immediately available to the COHERENT collaboration, with potentially more (up to ~ 9 tonnes) available in the future. The NaI[Tl] detectors are available in the form of 7.7-kg NaI[Tl] modules sealed in aluminum and packaged with Burle S83013 (or equivalent) photomultiplier tubes. These detectors have rectangular shapes and are suitable for deployment in a compact array. Their backgrounds have been characterized in the range ~ 200 counts $\text{keV}^{-1} \text{kg}^{-1} \text{day}^{-1}$ in the ~ 10 keV recoil energy range. The higher-energy ^{23}Na recoils should have better signal/background than ^{127}I recoils, so the focus is on these for the CEvNS measurement. Quenching factors have been measured to be $\sim 11\%$ [31], with recent measurements by COHERENT collaborators at TUNL favoring a larger $\sim 15\%$ value.

The potentially large mass of a detector to be deployed at the SNS also enables a search for CC interactions on ^{127}I , $\nu_e + ^{127}\text{I} \rightarrow e^- + ^{127}\text{Xe}^*$, which has a lower cross section than CEvNS on CsI by two orders of magnitude [19, 103], but which produces high-energy electrons (MeV scale) which are easily observable. The

ν_e cross section for interaction on ^{127}I , previously proposed for solar neutrino studies [24], has been measured previously with 34% uncertainty at a stopped-pion source [20]. Improved cross-section measurements of neutrino-induced interactions with significant momentum transfer could provide a new handle on possible g_A quenching, a matter of critical importance for future neutrinoless double-beta decay experiments (e.g., [104]). In particular, recent nuclear models predict a dependence of g_A quenching on momentum transfer (e.g., [105]) that could be tested with a stopped-pion neutrino source. We hope to make an improved measurement of the ^{127}I CC cross section and to explore the sensitivity of the NaI array to g_A -quenching physics. Future experiments using double-beta decay isotopes as targets could also provide interesting constraints on nuclear matrix element calculations [106].

The photomultiplier tubes packaged with the existing NaI[Tl] detectors have insufficient gain to observe a CEvNS signal with high efficiency. Hence, the Collaboration is refurbishing the PMT bases to allow higher-gain running, in order to enable observation of lower-energy recoils. A total of 185 kg of NaI[Tl] detectors have been deployed at the SNS (see Fig. 13) and have been running since November 2016 to measure backgrounds and explore CC interactions. Several upgrades, including improved shielding and cosmic-ray veto panels, have recently been completed. In the next phase, 2 tonnes will be deployed in high- or dual-gain mode with potential sensitivity to CEvNS signals as well as CC interactions. Although backgrounds are expected to be higher than for the other detectors, the large amount of target mass will provide large statistics.

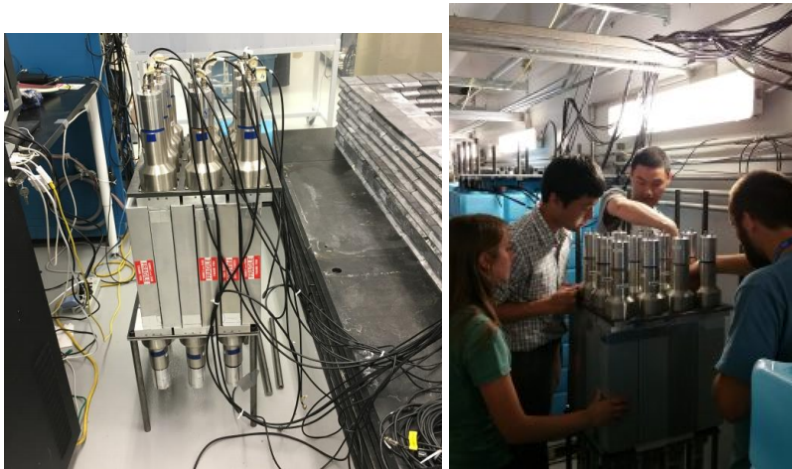


FIG. 13: Left: NaI[Tl] test stand at Duke University, showing individual detectors. Right: installation of the 185-kg NaI array in Neutrino Alley.

IV. COHERENT STATUS AND UPGRADES

As of this writing, the SNS-delivered protons on target for different COHERENT subsystems (corrected for detector livetime) are shown in Fig. 14.

The status of the four CEvNS detector subsystems at the time of this writing are as follows:

CsI[Na]: The detector was installed in 2015 and provided data for the first result in 2017 [1]. It will continue to run in the near future. Statistical uncertainties will be reduced, and we expect analysis improvements as well as improvement of quenching factor uncertainty from ancillary measurements.

LAr: The single-phase LAr scintillation detector was installed in Fall 2016 and took first beam in December 2016, running in that configuration through May 2017. It was upgraded for improved light yield for the next run period beginning July 2017. It will continue to run in that configuration into 2018.

NaI[Tl]: An initial deployment of 185 kg of NaI began data-taking in late 2016 in high-threshold mode (sensitive to CC on ^{127}I). Minor upgrades are ongoing, and refurbishment of PMT bases is underway to enable CEvNS running for additional detector deployment.

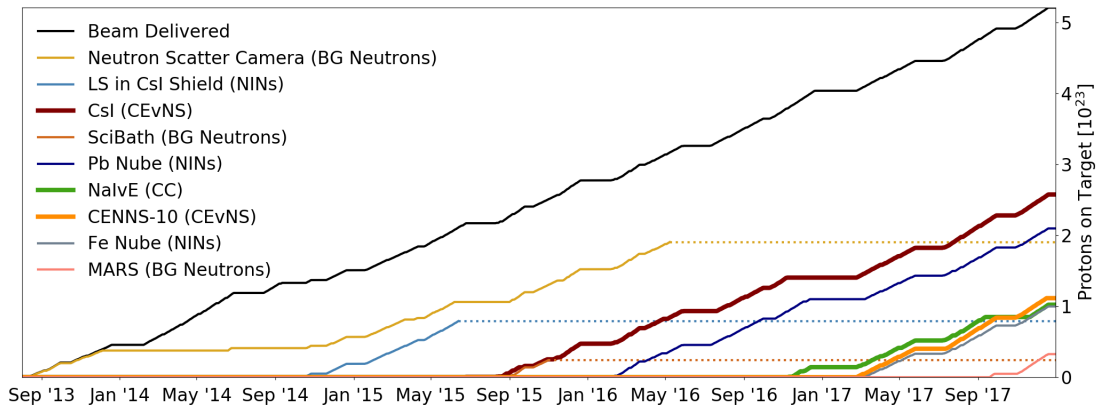


FIG. 14: Integrated protons on target from the SNS delivered to different COHERENT subsystems. The Neutron Scatter Camera and SciBath detectors are described in Sec. III B. The “LS in Csl Shield” line refers to the liquid scintillator cell deployed in the Csl detector shield described in Ref. [1]. The Pb and Fe Nubes are described in Sec. III B 2. “NaIvE (CC)” refers to the NaI[Tl] 185-kg detector running in low-gain CC mode as described in Sec. III C 4. “CENNS-10” refers to the single-phase liquid argon detector described in Sec. III C 3. “MARS” refers to the neutron detector described in Sec. III B.

Ge: The available Ge detectors are under test and refurbishment, with installation expected in 2018. The Collaboration is seeking to purchase and deploy additional detectors.

A. Future Upgrades

The COHERENT Collaboration is pursuing multiple possibilities for future upgrades to the suite of detectors in Neutrino Alley. Additional detector mass is under consideration for all existing targets except Csl[Na].

- A tonne-scale LAr detector is under consideration.
- Additional Ge detectors may be added to the existing apparatus.
- NaI[Tl] detectors, up to 9 tonnes, if available, may be added.

In addition, detectors employing different targets are also under consideration. There is benefit for physics sensitivity in measuring CEvNS with N values as different from each other as possible; a case in point is Ne and Xe, with greatly improved sensitivity to NSI [5]. Other nuclei are of interest for neutron-radius measurements [13].

Also under consideration by the Collaboration is “Mini-HALO” for a dedicated measurement of the NIN-production cross section and detection efficiency for the HALO experiment [21].

The dominant systematic uncertainty for many targets is due to the quenching factor uncertainty, and ancillary measurements are underway for independent measurements of these in the current COHERENT targets and others.

Although not dominant for the current Csl CEvNS measurement, uncertainties on the neutrino flux (currently $\sim 10\%$) will eventually become dominant. A current plan is to address this with heavy water, because the theoretical uncertainty for neutrino interactions on deuterons is small ($\sim 2 - 3\%$) [19, 107, 108]. A tonne-scale D₂O flux-monitoring detector is under design. Such a detector filled with regular water can also measure CC and NC interactions on ¹⁶O, of relevance to measurements of supernova neutrinos in Super-Kamiokande and Hyper-Kamiokande [109].

V. SUMMARY

In summary, the COHERENT program will take advantage of the extremely high-quality stopped-pion neutrino source available at the Spallation Neutron Source at Oak Ridge National Laboratory for new CEvNS measurements. Neutrino Alley in the basement of the SNS target building provides a unique low-background environment for neutrino experiments. Following the first measurement of CEvNS in CsI, four detector subsystems, based on CsI, Ge, Ar, and NaI, will demonstrate the N^2 dependence of the cross section and significantly improve constraints on non-standard interactions of neutrinos with nuclei. A secondary goal of COHERENT is to measure the cross sections for NINs on lead, iron, and potentially other targets, using independent scintillator detectors, in order to estimate the NIN component of the CEvNS detector signal. These measurements will be of interest in their own right to the nuclear-physics and particle-astrophysics communities, due to their relevance for supernova-neutrino detection. Beyond the current program, there is physics motivation for several potential upgrades, including increased mass for any of the existing targets, additional targets, and flux monitoring.

Acknowledgments

We acknowledge support from: the Alfred P. Sloan Foundation (BR2014-037), the Consortium for Non-proliferation Enabling Capabilities (de-na0002576), the Institute for Basic Science (Korea) (IBS-R017-G1-2017-a00), the National Science Foundation (PHY-1306942, PHY-1506357, PHY-1614545, HRD-1601174), Lawrence Berkeley National Laboratory Directed Research and Development funds, Russian Foundation for Basic Research (No. 17-02-01077_a), the Russian Science Foundation in the framework of MEPHI Academic Excellence Project (contract 02.a03.21.0005, 27.08.2013), Sandia National Laboratories Directed Research and Development Exploratory Express Funds, Triangle Universities Nuclear Laboratory, the U.S. Department of Energy Office of Science (de-sc0009824, de-sc0010007, Early Career Award de-sc0014249, de-sc0014558), Office of Science Graduate Student Research (SCGSR) program, the U.S. Department of Energy's National Nuclear Security Administration Office of Defense, Nuclear Nonproliferation Research, and Development, and the University of Washington Royalty Research Fund (FA124183). Sandia National Laboratories is a multimission laboratory managed and operated by National Technology and Engineering Solutions of Sandia LLC, a wholly owned subsidiary of Honeywell International Inc. for the U.S. Department of Energy's National Nuclear Security Administration under contract de-na0003525. This work was supported in part by the Kavli Institute for Cosmological Physics at the University of Chicago through grant NSF PHY-1125897, and an endowment from the Kavli Foundation and its founder Fred Kavli. This work was sponsored by the Laboratory Directed Research and Development Program of Oak Ridge National Laboratory, managed by UT-Battelle, LLC, for the U. S. Department of Energy. It used resources of the Spallation Neutron Source, which is a DOE Office of Science User Facility. This material is based upon work supported by the U.S. Department of Energy, Office of Science, Office of High Energy Physics. This research uses resources of the Oak Ridge Leadership Computing Facility, which is a DOE Office of Science User Facility. Raw experimental data are archived at its High Performance Storage System, which provides 263 TB of COHERENT dedicated storage. We are grateful for additional resources provided by the research computing centers at the University of Chicago, and Duke University. We thank Pacific Northwest National Laboratory colleagues for CsI[Na] detector contributions. We thank Fermilab for the loan of the CENNS-10 detector.

-
- [1] D. Akimov *et al.* (COHERENT). “Observation of Coherent Elastic Neutrino-Nucleus Scattering.” *Science* (2017). 1708.01294.
 - [2] D.Z. Freedman. “Coherent effects of a weak neutral current.” *Phys. Rev.* **D9**, 1389 (1974).
 - [3] V. B. Kopeliovich and L. L. Frankfurt. “Isotopic and chiral structure of neutral current.” *JETP Lett.* **19**, 145–147 (1974). [Pisma Zh. Eksp. Teor. Fiz.19,236(1974)].
 - [4] A. Drukier and L. Stodolsky. “Principles and applications of a neutral current detector for neutrino physics and astronomy.” *Phys. Rev.* **D30**, 2295 (1984).
 - [5] K. Scholberg. “Prospects for measuring coherent neutrino nucleus elastic scattering at a stopped-pion neutrino source.” *Phys. Rev.* **D73**, 033005 (2006). hep-ex/0511042.
 - [6] J. Barranco, O.G. Miranda, and T.I. Rashba. “Low energy neutrino experiments sensitivity to physics beyond the standard model.” *Phys. Rev.* **D76**, 073008 (2007). hep-ph/0702175.
 - [7] P. Coloma, P. B. Denton, M. C. Gonzalez-Garcia, M. Maltoni, and T. Schwetz. “Curtailling the Dark Side in Non-Standard Neutrino Interactions.” *JHEP* **04**, 116 (2017). 1701.04828.

- [8] P. Coloma, M. C. Gonzalez-Garcia, M. Maltoni, and T. Schwetz. “A COHERENT enlightenment of the neutrino Dark Side.” (2017). 1708.02899.
- [9] J. Liao and D. Marfatia. “COHERENT constraints on nonstandard neutrino interactions.” (2017). 1708.04255.
- [10] J.B. Dent, B. Dutta, S. Liao, J.L. Newstead, L.E. Strigari, and J.W. Walker. “Accelerator and reactor complementarity in coherent neutrino scattering.” (2017). 1711.03521.
- [11] T. S. Kosmas and D. K. Papoulias. “COHERENT constraints to conventional and exotic neutrino physics.” (2017). 1711.09773.
- [12] J. Billard, E. Figueroa-Feliciano, and L. Strigari. “Implication of neutrino backgrounds on the reach of next generation dark matter direct detection experiments.” *Phys. Rev.* **D89**, 023524 (2014).
- [13] M. Cadeddu, C. Giunti, Y. F. Li, and Y. Y. Zhang. “Average CsI neutron density distribution from COHERENT data.” (2017). 1710.02730.
- [14] J.R. Wilson. “Coherent Neutrino Scattering and Stellar Collapse.” *Phys. Rev. Lett.* **32**, 849 (1974).
- [15] K. Sato. “Supernova Explosion and Neutral Currents of Weak Interaction.” *Progress of Theoretical Physics* **54**, 1325–1338 (1975).
- [16] C.J. Horowitz, M.A. Perez-Garcia, J. Carriere, D.K. Berry, and J. Piekarewicz. “Nonuniform neutron-rich matter and coherent neutrino scattering.” *Phys. Rev.* **C70**, 065806 (2004). astro-ph/0409296.
- [17] C.J. Horowitz, K.J. Coakley, and D.N. McKinsey. “Supernova observation via neutrino nucleus elastic scattering in the CLEAN detector.” *Phys. Rev.* **D68**, 023005 (2003). astro-ph/0302071.
- [18] S. Chakraborty, P. Bhattacharjee, and K. Kar. “Observing supernova neutrino light curve in future dark matter detectors.” *Phys. Rev.* **D89**, 013011 (2014). 1309.4492.
- [19] J. A. Formaggio and G. P. Zeller. “From eV to EeV: Neutrino Cross Sections Across Energy Scales.” *Rev. Mod. Phys.* **84**, 1307–1341 (2012). 1305.7513.
- [20] J. R. Distel, B. T. Cleveland, K. Lande, C. K. Lee, P. S. Wildenhain, G. E. Allen, and R. L. Burman. “Measurement of the cross-section for the reaction I-127 ($\nu(e), e^-$) Xe-127(bound states) with neutrinos from the decay of stopped muons.” *Phys. Rev.* **C68**, 054613 (2003). nucl-ex/0208012.
- [21] C.A. Duba, F. Duncan, J. Farine, A. Habig, A. Hime, *et al.* “HALO: The helium and lead observatory for supernova neutrinos.” *J. Phys. Conf. Ser.* **136**, 042077 (2008).
- [22] S.E. Woosley, D.H. Hartmann, R.D. Hoffman, and W.C. Haxton. “The ν -process.” *Astrophys. J.* **356**, 272–301 (1990).
- [23] Y.-Z. Qian, W.C. Haxton, K. Langanke, and P. Vogel. “Neutrino-induced neutron spallation and supernova r-process nucleosynthesis.” *Phys. Rev.* **C55**, 1532 (1997).
- [24] W. C. Haxton. “Radiochemical neutrino detection via $127\text{I}(\nu e, e^-)127\text{Xe}$.” *Physical Review Letters* **60**, 768–771 (1988).
- [25] D. Akimov *et al.* (COHERENT). “The COHERENT Experiment at the Spallation Neutron Source.” (2015). 1509.08702.
- [26] J. Barranco, O.G. Miranda, and T.I. Rashba. “Probing new physics with coherent neutrino scattering off nuclei.” *J. High Energy Phys.* **2005**, 021 (2005). hep-ph/0508299.
- [27] K.A. Olive *et al.* “Review of Particle Physics.” *Chin. Phys. C* **38**, 090001 (2014).
- [28] R. Helm. “Inelastic and Elastic Scattering of 187-Mev Electrons from Selected Even-Even Nuclei.” *Physical Review* **104**, 1466–1475 (1956).
- [29] R. Hofstadter. “Electron scattering and nuclear structure.” *Rev. Mod. Phys.* **28**, 214–254 (1956).
- [30] S. Klein and J. Nystrand. “Exclusive vector meson production in relativistic heavy ion collisions.” *Phys.Rev.* **C60**, 014903 (1999). hep-ph/9902259.
- [31] J.I. Collar. “Quenching and Channeling of Nuclear Recoils in NaI[Tl]: Implications for Dark Matter Searches.” *Phys. Rev.* **C88**, 035806 (2013). 1302.0796.
- [32] L.M. Krauss. “Low-energy neutrino detection and precision tests of the standard model.” *Phys. Lett.* **B269**, 407–411 (1991).
- [33] R. Harnik, J. Kopp, and P.A.N. Machado. “Exploring ν Signals in Dark Matter Detectors.” *JCAP* **1207**, 026 (2012). 1202.6073.
- [34] B. Dutta, R. Mahapatra, L. E. Strigari, and J.W. Walker. “Sensitivity to Z-prime and non-standard neutrino interactions from ultra-low threshold neutrino-nucleus coherent scattering.” (2015). 1508.07981.
- [35] J. Dorenbosch *et al.* (CHARM). “Experimental verification of the universality of electron-neutrino and muon-neutrino coupling to the neutral weak current.” *Phys. Lett.* **B180**, 303 (1986).
- [36] P. Coloma and T. Schwetz. “Generalized mass ordering degeneracy in neutrino oscillation experiments.” *Phys. Rev.* **D94**, 055005 (2016). [Erratum: *Phys. Rev.*D95,no.7,079903(2017)], 1604.05772.
- [37] B. Cabrera, L.M. Krauss, and F. Wilczek. “Bolometric Detection of Neutrinos.” *Phys.Rev.Lett.* **55**, 25 (1985).
- [38] J. Monroe and P. Fisher. “Neutrino Backgrounds to Dark Matter Searches.” *Phys. Rev.* **D76**, 033007 (2007). 0706.3019.
- [39] A. Gütlein, C. Ciemiak, F. von Feilitzsch, N. Haag, M. Hofmann, *et al.* “Solar and atmospheric neutrinos: Background sources for the direct dark matter search.” *Astropart. Phys.* **34**, 90–96 (2010). 1003.5530.
- [40] P. Cushman *et al.* “Snowmass CF1 Summary: WIMP Dark Matter Direct Detection.” (2013). 1310.8327.

- [41] A.J. Anderson, J.M. Conrad, E. Figueroa-Feliciano, K. Scholberg, and J. Spitz. “Coherent neutrino scattering in dark matter detectors.” *Phys. Rev.* **D84**, 013008 (2011).
- [42] A. Gütlein *et al.* “Impact of coherent neutrino nucleus scattering on direct dark matter searches based on CaWO_4 crystals.” *Astropart. Phys.* **69**, 44–49 (2015). 1408.2357.
- [43] J. Billard, L.E. Strigari, and E. Figueroa-Feliciano. “Solar neutrino physics with low-threshold dark matter detectors.” *Phys. Rev.* **D91**, 095023 (2015). 1409.0050.
- [44] C. E. Aalseth *et al.* “DarkSide-20k: A 20 Tonne Two-Phase LAr TPC for Direct Dark Matter Detection at LNGS.” (2017). 1707.08145.
- [45] P. A. Amaudruz *et al.* (DEAP-3600). “First results from the DEAP-3600 dark matter search with argon at SNOLAB.” (2017). 1707.08042.
- [46] R. Agnese *et al.* (SuperCDMS Collaboration). “Search for Low-Mass Weakly Interacting Massive Particles with SuperCDMS.” *Phys. Rev. Lett.* **112**, 241302 (2014).
- [47] E. Armengaud *et al.* (EDELWEISS). “Performance of the EDELWEISS-III experiment for direct dark matter searches.” *JINST* **12**, P08010 (2017). 1706.01070.
- [48] W. Zhao *et al.* (CDEX). “Search of low-mass WIMPs with a p -type point contact germanium detector in the CDEX-1 experiment.” *Phys. Rev.* **D93**, 092003 (2016). 1601.04581.
- [49] R. Bernabei *et al.* (DAMA). “The DAMA/LIBRA apparatus.” *Nucl. Instrum. Meth.* **A592**, 297–315 (2008). 0804.2738.
- [50] J. Chervinka *et al.* (DM-Ice17). “First data from DM-Ice17.” *Phys. Rev.* **D90**, 092005 (2014). 1401.4804.
- [51] C. Tomei (SABRE). “SABRE: Dark matter annual modulation detection in the northern and southern hemispheres.” *Nucl. Instrum. Meth.* **A845**, 418–420 (2017).
- [52] G. Adhikari *et al.* “Design and Initial Performance of the COSINE-100 Experiment.” (2017). 1710.05299.
- [53] S.C. Kim *et al.* (KIMS Collaboration). “New Limits on Interactions between Weakly Interacting Massive Particles and Nucleons Obtained with CsI(Tl) Crystal Detectors.” *Phys. Rev. Lett.* **108**, 181301 (2012).
- [54] G.W. Bennet (Muon $g-2$ Collaboration). “Final report of the E821 muon anomalous magnetic moment measurement at BNL.” *Phys. Rev.* **D73**, 072003 (2006).
- [55] F. Jegerlehner and A. Nyffeler. “The muon $g-2$.” *Phys. Rept.* **477**, 1–110 (2009).
- [56] H. Davoudiasl, H.-S. Lee, and W.J. Marciano. “Muon Anomaly and Dark Parity Violation.” *Phys. Rev. Lett.* **109**, 031802 (2012).
- [57] H. Davoudiasl, H.-S. Lee, and W.J. Marciano. ““Dark” Z implications for parity violation, rare meson decays, and Higgs physics.” *Phys. Rev.* **D85**, 115019 (2012).
- [58] H. Davoudiasl, H.-S. Lee, and W.J. Marciano. “Muon $g-2$, rare kaon decays, and parity violation from dark bosons.” *Phys. Rev.* **D89**, 095006 (2014).
- [59] K.S. Kumar, S. Mantry, W.J. Marciano, and P.A. Souder. “Low Energy Measurements of the Weak Mixing Angle.” *Annu. Rev. Nucl. Part. Sci.* **63**, 237–267 (2013).
- [60] J. Erler, C.J. Horowitz, S. Mantry, and P.A. Souder. “Weak Polarized Electron Scattering.” *Ann.Rev.Nucl.Part.Sci.* **64**, 269–298 (2014).
- [61] A.C. Dodd, E. Papageorgiu, and S. Ranfone. “The effect of a neutrino magnetic moment on nuclear excitation processes.” *Phys. Lett.* **B266**, 434–438 (1991).
- [62] T.S. Kosmas, O.G. Miranda, D.K. Papoulias, M. Tortola, and J.W.F. Valle. “Probing neutrino magnetic moments at the Spallation Neutron Source facility.” *Phys. Rev.* **D92**, 013011 (2015). 1505.03202.
- [63] J. Papavassiliou, J. Bernabeu, and M. Passera. “Neutrino-nuclear coherent scattering and the effective neutrino charge radius.” *PoS HEP2005*, 192 (2006). hep-ph/0512029.
- [64] C. Giunti and M. Laveder. “Short-Baseline Active-Sterile Neutrino Oscillations?” *Mod. Phys. Lett.* **A22**, 2499–2509 (2007). hep-ph/0610352.
- [65] P.S. Amanik and G.C. McLaughlin. “Nuclear neutron form factor from neutrino nucleus coherent elastic scattering.” *J. Phys.* **G36**, 015105 (2009).
- [66] K. Patton, J. Engel, G.C. McLaughlin, and N. Schunck. “Neutrino-nucleus coherent scattering as a probe of neutron density distributions.” *Phys. Rev.* **C86**, 024612 (2012). 1207.0693.
- [67] O. Moreno and T.W. Donnelly. “A unified approach to electron and neutrino elastic scattering off nuclei with an application to the study of the axial structure.” (2015). 1506.04733.
- [68] P. deNiverville, M. Pospelov, and A. Ritz. “Light new physics in coherent neutrino-nucleus scattering experiments.” (2015). 1505.07805.
- [69] S.-F. Ge and I. M. Shoemaker. “Constraining Photon Portal Dark Matter with TEXONO and COHERENT Data.” (2017). 1710.10889.
- [70] A. Bolozdynya, F. Cavanna, Y. Efremenko, G.T. Garvey, V. Gudkov, *et al.* “Opportunities for Neutrino Physics at the Spallation Neutron Source: A White Paper.” (2012). 1211.5199.
- [71] S. Agostinelli *et al.* (GEANT4). “GEANT4: A simulation toolkit.” *Nucl. Instrum. Meth.* **A506**, 250–303 (2003).
- [72] S.J. Brice, R.L. Cooper, F. DeJongh, A. Empl, L.M. Garrison, *et al.* “A New Method for Measuring Coherent Elastic Neutrino Nucleus Scattering at an Off-Axis High-Energy Neutrino Beam Target.” *Phys. Rev.* **D89**,

- 072004 (2014). 1311.5958.
- [73] M. Harada *et al.* (JSNS2). “Proposal: A Search for Sterile Neutrino at J-PARC Materials and Life Science Experimental Facility.” (2013). 1310.1437.
- [74] S. Axani, G. Collin, J.M. Conrad, M.H. Shaevitz, J. Spitz, and T. Wongjirad. “A Decisive Disappearance Search at High- Δm^2 with Monoenergetic Muon Neutrinos.” (2015). 1506.05811.
- [75] N. Mascarenhas, J. Brennan, K. Krenz, P. Marleau, and S. Mrowka. “Results With the Neutron Scatter Camera.” *IEEE Trans. Nucl. Sci.* **56**, 1269 (2009).
- [76] R. Tayloe, H.O. Meyer, D.C. Cox, J. Doskow, A. Ferguson, T. Katori, M. Novak, and D. Passmore. “A large-volume detector capable of charged-particle tracking.” *Nucl. Instrum. Meth.* **A562**, 198–206 (2006).
- [77] R. Cooper, L. Garrison, H.O. Meyer, T. Mikev, L. Rebenitsch, and R. Tayloe. “SciBath: A Novel Tracking Detector for Measuring Neutral Particles Underground.” *In Particles and fields. Proc. DPF 2011, Providence, USA, August 9-13, 2011* (2011). 1110.4432.
- [78] C. Roecker, A. Bernstein, N. S. Bowden, B. Cabrera-Palmer, S. Dazeley, M. Gerling, P. Marleau, M. D. Sweany, and K. Vetter. “Design of a transportable high efficiency fast neutron spectrometer.” *Nucl. Instrum. Meth.* **A826**, 21–30 (2016).
- [79] G.M. Fuller, W.C. Haxton, and G.C. McLaughlin. “Prospects for detecting supernova neutrino flavor oscillations.” *Phys. Rev.* **D59**, 085005 (1999). astro-ph/9809164.
- [80] E. Kolbe and K. Langanke. “The Role of neutrino induced reactions on lead and iron in neutrino detectors.” *Phys.Rev.* **C63**, 025802 (2001). nucl-th/0003060.
- [81] J. Engel, G.C. McLaughlin, and C. Volpe. “What can be learned with a lead based supernova neutrino detector?” *Phys. Rev.* **D67**, 013005 (2003). hep-ph/0209267.
- [82] R. Maschuw. “Neutrino spectroscopy with KARMEN.” *Progress in Particle and Nuclear Physics* **40**, 183–192 (1998).
- [83] D. Väänänen and C. Volpe. “The neutrino signal at HALO: learning about the primary supernova neutrino fluxes and neutrino properties.” *JCAP* **2011**, 019 (2011). 1105.6225.
- [84] J.I. Collar *et al.* “Coherent neutrino-nucleus scattering detection with a CsI [Na] scintillator at the SNS spallation source.” *Nucl. Instrum. Meth.* **A773**, 56–65 (2015).
- [85] B. Scholz. *First observation of coherent elastic neutrino-nucleus scattering*. Ph.D. thesis, University of Chicago (2017).
- [86] G. Rich. *Measurement of low-energy nuclear-recoil quenching factors in CsI[Na] and statistical analysis of the first observation of coherent, elastic neutrino-nucleus scattering*. Ph.D. thesis, University of North Carolina, Chapel Hill (2017).
- [87] P.S. Barbeau, J.I. Collar, and O. Tench. “Large-Mass Ultra-Low Noise Germanium Detectors: Performance and Applications in Neutrino and Astroparticle Physics.” *JCAP* **0709**, 009 (2007). nucl-ex/0701012.
- [88] P.S. Barbeau. *Neutrino and Astroparticle Physics with P-Type Point Contact High Purity Germanium Detectors*. Ph.D. thesis, U. Chicago (2009). Ph.D. thesis, AAT-3386971.
- [89] C. E. Aalseth, P. S. Barbeau, *et al.* (CoGeNT Collaboration). “Experimental Constraints on a Dark Matter Origin for the DAMA Annual Modulation Effect.” *Phys. Rev. Lett.* **101**, 251301 (2008). URL <https://link.aps.org/doi/10.1103/PhysRevLett.101.251301>.
- [90] C. E. Aalseth, P. S. Barbeau, *et al.* (CoGeNT Collaboration). “Results from a Search for Light-Mass Dark Matter with a p-Type Point Contact Germanium Detector.” *Phys. Rev. Lett.* **106**, 131301 (2011). URL <https://link.aps.org/doi/10.1103/PhysRevLett.106.131301>.
- [91] C.E. Aalseth, P.S. Barbeau, J. Colaresi, J.I. Collar, J. Diaz Leon, *et al.* “Search for an Annual Modulation in a P-type Point Contact Germanium Dark Matter Detector.” *Phys. Rev. Lett.* **107**, 141301 (2011). 1106.0650.
- [92] C.E. Aalseth *et al.* (CoGeNT Collaboration). “CoGeNT: A Search for Low-Mass Dark Matter using p-type Point Contact Germanium Detectors.” *Phys. Rev.* **D88**, 012002 (2013). 1208.5737.
- [93] N. Abgrall, E. Aguayo, F.T. Avignone III, *et al.* “The MAJORANA DEMONSTRATOR Neutrinoless Double-Beta Decay Experiment.” *Advances in High Energy Physics* **2014** (2014).
- [94] The GERDA Collaboration. “Background-free search for neutrinoless double-decay of 76Ge with GERDA.” *Nature* **544**, 47 EP – (2017). URL <http://dx.doi.org/10.1038/nature21717>.
- [95] S.T. Lin *et al.* “New limits on spin-independent and spin-dependent couplings of low-mass WIMP dark matter with a germanium detector at a threshold of 220 eV.” *Phys. Rev.* **D79**, 061101 (2009).
- [96] M. Lindner, W. Rodejohann, and X. Xu. “Coherent neutrino-nucleus scattering and new neutrino interactions.” *Journal of High Energy Physics* **2017**, 97 (2017). ISSN 1029-8479. URL [https://doi.org/10.1007/JHEP03\(2017\)097](https://doi.org/10.1007/JHEP03(2017)097).
- [97] J. Hakenmuller. “CONUS: Towards the detection of coherent elastic neutrino nucleus scattering.” Presentation at TAUP 2017. Available from <https://indico.cern.ch/event/606690/contributions/2591545/>.
- [98] D.Yu. Akimov *et al.* (RED). “Prospects for observation of neutrino-nuclear neutral current coherent scattering with two-phase Xenon emission detector.” *JINST* **8**, P10023 (2013). 1212.1938.
- [99] K. Scholberg, T. Wongjirad, E. Hungerford, A. Empl, D. Markoff, *et al.* “The CLEAR Experiment.” (2009). 0910.1989.

- [100] M.G. Boulay and A. Hime. “Technique for direct detection of weakly interacting massive particles using scintillation time discrimination in liquid argon.” *Astropart.Phys.* **25**, 179–182 (2006).
- [101] R. Tayloe (COHERENT). “The CENNS-10 Liquid Argon Detector to measure CEvNS at the Spallation Neutron Source.” In *Light Detection in Noble Elements (LIDINE 2017) Menlo Park, CA, USA, September 22-24, 2017* (2017). 1801.00086, URL <http://inspirehep.net/record/1645626/files/arXiv:1801.00086.pdf>.
- [102] H. Cao *et al.* (SCENE). “Measurement of Scintillation and Ionization Yield and Scintillation Pulse Shape from Nuclear Recoils in Liquid Argon.” *Phys. Rev.* **D91**, 092007 (2015). 1406.4825.
- [103] J. Engel, S. Pittel, and P. Vogel. “Capture of solar and higher energy neutrinos by I-127.” *Phys. Rev.* **C50**, 1702–1708 (1994). nucl-th/9402022.
- [104] J. Engel and J. Menendez. “Status and Future of Nuclear Matrix Elements for Neutrinoless Double-Beta Decay: A Review.” *Rept. Prog. Phys.* **80**, 046301 (2017). 1610.06548.
- [105] J. Menendez, D. Gazit, and A. Schwenk. “Chiral two-body currents in nuclei: Gamow-Teller transitions and neutrinoless double-beta decay.” *Phys. Rev. Lett.* **107**, 062501 (2011). 1103.3622.
- [106] C. Volpe. “Neutrino-nucleus interactions as a probe to constrain double-beta decay predictions.” *J. Phys.* **G31**, 903–908 (2005). hep-ph/0501233.
- [107] Yu. V. Kozlov, S. V. Khalturtsev, I. N. Machulin, A. V. Martemyanov, V. P. Martemyanov, S. V. Sukhotin, V. G. Tarasenkov, E. V. Turbin, and V. N. Vyrodov. “Anti-neutrino deuteron experiment at Krasnoyarsk.” *Phys. Atom. Nucl.* **63**, 1016–1019 (2000). [Yad. Fiz.63,1091(2000)], hep-ex/9912047.
- [108] S. Nakamura, T. Sato, S. Ando, T. S. Park, F. Myhrer, Vladimir P. Gudkov, and K. Kubodera. “Neutrino deuteron reactions at solar neutrino energies.” *Nucl. Phys.* **A707**, 561–576 (2002). nucl-th/0201062.
- [109] K. Scholberg. “Supernova Neutrino Detection.” *Ann.Rev.Nucl.Part.Sci.* **62**, 81–103 (2012). 1205.6003.